International Journal on Advanced Science Engineering Information Technology

Vol.10 (2020) No. 1
ISSN: 2088-5334

Mathematical Models Selection on the Total Suspended Solid Mapping using Reflective Satellite Image Data

Hendrata Wibisana[#], Bangun Muljo S[*], Umboro Lasminto[+]

[#]*Post-Graduate Program, Geomatic Engineering, Sepuluh Nopember Institute of Technology, Keputih Sukolilo, Surabaya, 60111, Indonesia*
E-mail: hendrata2008@gmail.com

[*]*Geomatic Engineering Department, Sepuluh Nopember Institute of Technology, Keputih Sukolilo, Surabaya, 60111, Indonesia*
E-mail: bangun.ms@gmail.com

[+]*Civil Engineering Department , Sepuluh Nopember Institute of Technology, Keputih Sukolilo , Surabaya, 60111,Indonesia*
E-mail: umboro.lasminto@gmail.com

***Abstract*— Ujung Pangkah Gresik is a reasonably dynamic area in the growth of turbidity levels in coastal beaches. As an area that has the estuary of the River Bengawan Solo, then Ujung Pangkah each year will experience the sedimentation process, one of which is the result of the movement of the river flow. This study aims to find the best mathematical model as an illustration of the total dynamics of the dissolved solids occurring in the area. The method used is a linear regression analysis of several selected models such as linear model, exponent, logarithm, polynomial degree 2, polynomial degree 3 and power model. The independent variable used in this research is the reflectance value of the Aqua Modis Level 2 from satellite imagery at wavelength 412 nm, 531 nm, and 645 nm. The results obtained from this study are the ability of Aqua Modis satellite imagery in mapping the total suspended solids, besides that it can also be used to predict changes in the total value of suspended solids by calculating remote sensing algorithms that produce optimal mathematical models, where the model used is the polynomial model degree 3 and the logarithmic model based on choosing a high correlation value of the model that is 0.75 obtained at a wavelength of 645 nanometers**

***Keywords*— Aqua Modis mathematical model; reflectance; total suspended solids.**

I. INTRODUCTION

Reflectance from satellite imagery is one of the variables that are needed to detect climate change from the ecosystem existing in an area.[1] Reflectance is the result of electromagnetic radiation emitted by an object when the object is exposed to sunlight which is the primary energy source. The exposure of sunlight in his journey on the surface of the earth, some of which is absorbed and some are reflected back. The magnitude of the reflected or reflectance value of each object affected by solar radiation is not the same. This is a characteristic of each object. The soil, rocks, water and foliage have their characteristics in reflecting the energy of sunlight that is about itself. From the phenomenon, the reflectance value has been widely used by remote sensing experts as a variable for the detection of natural resources that exist on the surface of the earth and the changes that occur in the earth's atmosphere [2]–[4].

One of the benefits of the widely used reflectance is to detect turbidity occurring in a water body, primarily in the river and coastal streams [5]. The flow of the river at any time in its journey from upstream to downstream will bring with it dissolved solids. The number of dissolved solids carried depends on the number of sedimentation processes occurring along the existing river body, as well as the flow rate of the river.

Total soluble solids is one of the water quality parameters that have been widely researched by remote sensing experts in addition to other parameters such as chlorophyll-a [6]–[8], sea surface temperature [9], salinity [10], using various instruments such as Meris [11]–[14], ALOS and Aster [15], SPOT [16], Landsat 5 [17], Landsat 7 [18], Landsat 8 [19] and Aqua Modis [20]–[22].

Robabeh et all.[23] has been doing this research about total suspended solids in the Penang area; they used THEOS satellite images to measured the content of TSS to get the water quality. Statistical models are used to obtain an overview of water quality with in-situ data; a multispectral algorithm is used to map water quality with the aim of better environmental quality management.

The main reason underlying this research is the mathematical models used by researchers often only provide

the best results for linear and exponential mathematical models without including the results for other mathematical models, so researchers only know the best results without knowing the results for the other model whether does it provide a wrong correlation value with a high standard of error

This research aims to achieve the best mathematical model from the total growth process of dissolved solids in the Ujung Pangkah Gresik coast. As the independent variable is taken the reflecting value of the Aqua Modis satellite image, where this value is obtained by extraction at a visible wavelength of wavelength 412 nm, 531 nm, and 645 nm.

II. Materials and Method

A. Research Location

The location in this research took place at Ujung Pangkah Gresik, where this location is the boundary with the Java Sea in the north, Madura Island in the east, Lamongan district in the west and Surabaya city in the south. The location of this study is limited by the latitude and longitude coordinates which map the study location so that the sample data used can be determined more precisely. The coordinates are 112o 30 'E to 113o 20' E for longitude and 6o 30 'S to 7o S for latitude, as seen in Figure 1.

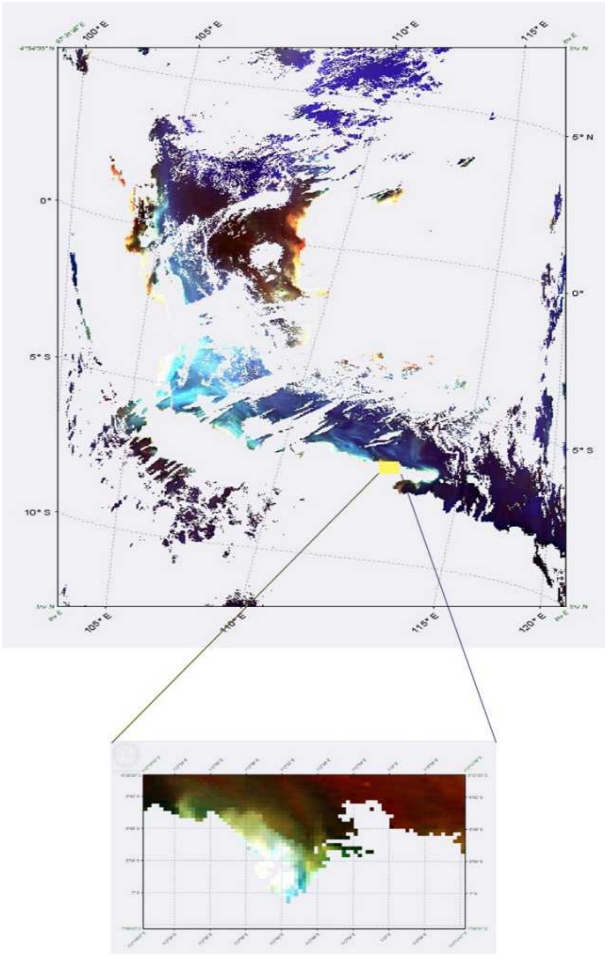

Fig 1. Image of research location at Ujung Pangkah Gresik

B. Satellite Image

Satellite images that used in this research are Aqua Modis with the name of the file is A2017215061500. L2_LAC_OC.nc which retrieved on a date 3 August 2017 on the webpage http://oceandata.sci.gsfc.nasa.gov, these satellite images have a 1 km spatial resolution which carried on Aqua platform with Modi's instrument and has processing level L2. Images of Aqua Modis which have been retrieved can be seen in Figure 1.

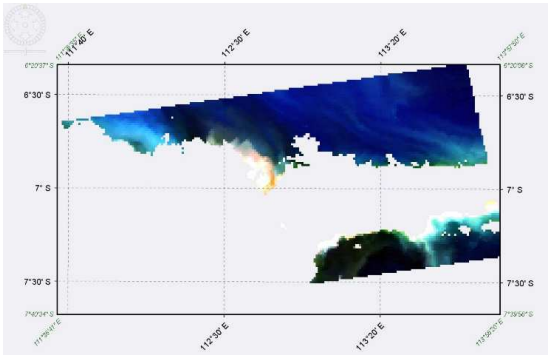

Fig 2. Display of satellite imagery after the process of reprojection

Figure 1. shows the images of the edge of Ujung Pangkah Gresik and surrounding areas, Aqua Modis is satellite images with a low resolution of 1 km, but with this resolution, it can map existing natural resources over a large area as shown in Figure 1., where boundaries of satellite imagery swept the area of Gresik and Madura islands. This satellite image still needs to be corrected further and for that to be reprocessed and with the SeaDASS process can be done such process as seen in Figure 2.

The result of satellite image reprojection, as shown in Figure 2, has a rectification of the image layout and adjustment of the existing coordinates. The reprojection process carried out on satellite imagery as shown in Figure 2 is continued by rearranging the composition of the map image of the study location. The rearrangement in question is carried out further cuts to produce a more representative picture of the location and the results are given in Figure 3.

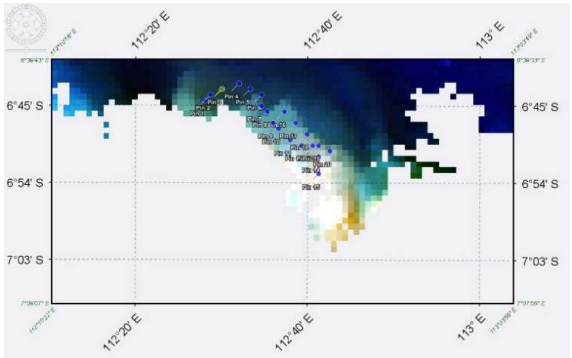

Fig 3. Point of coordinate for sample data of TSS

Furthermore from Figure 3 the coordinates of the sampling point are given which are scattered as much as 20 sample data From the sample data, 15 data are used to find the most optimal mathematical model using the remote sensing algorithm, then the mathematical model that has been formed and selected based on the largest R correlation

value will be used for validation calculations by entering the remaining sample data (5 data that are exist) into the mathematical model as an independent variable so that later the total value of dissolved solids from the results will be obtained which will be compared with in situ data or field data. The suitability of the mathematical model used in the distribution of the total value of dissolved solids will be seen from the magnitude of the RMSE value calculated from the TSS in the field with the TSS from the validation calculation.

C. Measurement of Total Suspended Solid

The seawater extract at the designated point by handheld GPS was then taken to the laboratory, and Gravimetric analysis is performed to determine the TSS content in milligrams per liter of sample water [24]. The result of measurement after drying with the oven is shown in Table 1 which contains TSS (total suspended solids) data according to the coordinates paper must use a page size corresponding to A4 which is 210mm (8.27") wide and 297mm (11.69") long.

D. Algorithm for Total Suspended Solid

To find the best mathematical model, a series of calculations were performed using several standard models owned by the Excel program, and from the model, the most optimum correlation value for each model was taken so that from the R correlation value the best model that could be considered for used as a model that describes the mathematical relationship between the reflectance of satellite images and the concentration of TSS obtained in the field.

The model used to find the algorithm for mapping total suspended solid is a linear model, exponential model, logarithmic, polynomial, and power model. with the trend analysis obtained the same mathematical model and the correlation value R, and this calculation is done for each wavelength available at Aqua MODIS namely wavelength 412, wavelength 531 and wavelength 645

III. Results and Discussion

A. Total Suspended Solid Data

The results of measurement for total suspended solid concentration from field sample data are given as follows (as seen in Table 1.)

TABLE I
DATA OF TSS (MG/L) FROM SAMPLE POINT AT UJUNG PANGKAH GRESIK

Latitude	Longitude	TSS (mg/l)
-6° 45’ 17.298”	112° 27’ 09.98”	48.5
-6° 44’ 37.559”	112° 27’ 49.50”	44.9
-6° 43’ 57.701”	112° 29’ 08.70”	24.7
-6° 12’ 56.844”	112° 31’ 07.48”	26.2
-6° 43’ 57.086”	112° 32’ 26.88”	54.9
-6° 44’ 36.452”	112° 33’ 46.29”	64.3
-6° 45’ 55.721”	112° 33’ 46.56”	61.5
-6° 46’ 35.210”	112° 34’ 26.32”	60.8
-6° 47’ 54.349”	112° 35’ 06.25”	66.2
-6° 48’ 33.835”	112° 35’ 46.01”	63.4
-6° 49’ 52.837”	112° 37’ 05.59”	82.4
-6° 50’ 32.185”	112° 38’ 25.01”	65.7
-6° 50’ 31.914”	112° 39’ 44.31”	52.8
-6° 51’ 51.040”	112° 40’ 24.20”	48.5
-6° 53’ 49.919”	112° 40’ 24.65”	78.3

From the data generated in Table 1 and by combining the satellite image reflectance data at the wavelength of 412 nm, 531 nm and 645 nm, the mathematical model can be produced by calculation using linear regression method, mathematical model and coefficient of determination R for 412 nm wavelength seen in Table 2, whereas seen in the table the most suitable model with the highest R-value is the polynomial model of degree 3.

Fig 4 shows a composite color of satellite images from Aqua MODIS for wavelengths 412, 531 and 645 nm. Moreover, by setting the RGB band with the sequence composition then the composite color obtained for A with the sequence 645-531-412, where the wavelength 645 is red, 531 is green and 412 is blue, while for composite color B is the arrangement for the order 412-531- 645 and composite C color is generated from the sequence settings 531-412-645. The purpose of setting the composite color is to get an initial picture of the satellite image spectral by looking at the situation in the Ujung Pangkah Gresik area.

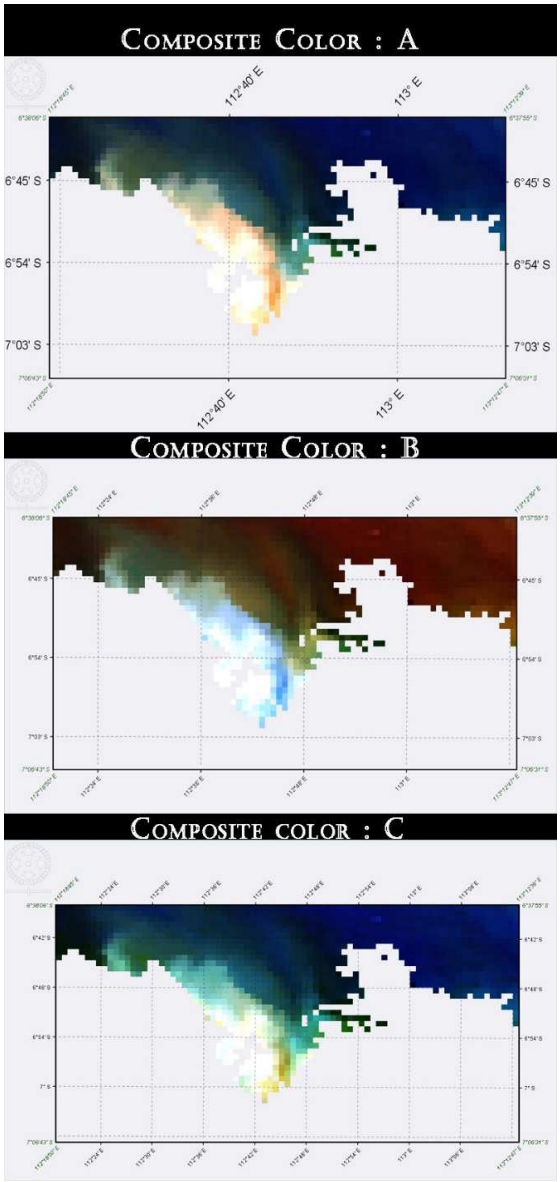

Fig 4. Composite color of each wavelength, where [A] 645-531-412; [B] 412-531-645 and [C] 531-412-645

B. *Mathematical Model From Remote Sensing Algorithm*

The result of a mathematical model for wavelength 531 nm toward the value of total suspended solid can be seen in Table 3, where the data in the table can be seen that the most suitable model with the highest determinant coefficient value R is the polynomial model 3 with R = 0.713. Table 4. represents the processing of a mathematical model with the coefficient value R for a wavelength of 645 nm, wherein the table it is shown that the most suitable model is a polynomial model of 3 with R = 0.7452. The only interesting for Table 4 is that the overall mathematical model generated has a value of R coefficient above 0.5 which means that statistically, 50% of the data can be represented on a linear regression line. This is in contrast with the Table 2 and also Table 3, where for both tables the wavelength 412 and wavelength 531 nm results obtained in the mathematical model do not all have R above 0.5, just for Table 2 all of the existing models have a value R is relatively low in the absence of a mathematical model that has a value of R above 0.5 so it can be said that for the wavelength 412 nm is less contribute to the mapping concentration of TSS in the field.

TABLE II
THE MATHEMATICAL BUILDING OF RRS_412 NM REFLECTANCE WITH TSS CONCENTRATION

No	Model	Mathematic equation	R^2
1	Linier	TSS = -5666.2*Rrs_412 + 95.521	0.2906
2	Exponent	$TSS = 119.78e^{-116,1*Rrs\_412}$	0.2682
3	Logarithmic	TSS = -39.74ln(Rrs_412) – 142.28	0.3129
4	Polynomial 2	$TSS = 3E+06*(Rrs\_412)^2 – 43257*(Rrs\_412) + 220.18$	0.3763
5	Polynomial 3	$TSS = 6E+08*(Rrs\_412)^3 - 1E+07*(Rrs\_412)^2 + 47654*(Rrs\_412) + 15.092$	0.3867
6	Power	$TSS = 0.9342*(Rrs\_412)^{-0,811}$	0.2861

TABLE III
THE MATHEMATICAL BUILDING OF RRS_531 NM REFLECTANCE WITH TSS CONCENTRATION

No	Model	Mathematic equation	R^2
1	Linier	TSS = -1723.8*(Rrs_531) + 70.434	0.1788
2	Exponent	$TSS = 72.688e^{-37,08*Rrs\_531}$	0.1819
3	Logaritmic	TSS = -15.77ln(Rrs_531) – 21.31	0.2541
4	Polynomial 2	$TSS = 847903*(Rrs\_531)^2 – 16484*(Rrs\_531) + 121.97$	0.5820
5	Polynomial 3	$TSS = 2E+08*(Rrs\_531)^3 - 5E+06*(Rrs\_531)^2 + 33423*(Rrs\_531) – 2.435$	0.7130
6	Power	$TSS = 10.469*(Rrs\_531)^{-0.332}$	0.2475

TABLE IV
THE MATHEMATICAL BUILDING OF RRS_645 NM REFLECTANCE WITH TSS CONCENTRATION

No	Model	Mathematic equation	R^2
1	Linier	TSS = 8154,1*Rrs_645 + 35,364	0.5680
2	Exponent	$TSS = 35,165e^{164,33*Rrs\_645}$	0.5072
3	Logaritmic	TSS = 21,088*ln(Rrs_645) + 185,79	0.6829
4	Polynomial 2	$TSS = -3E+06*(Rrs\_645)^2 + 23661*(Rrs\_645) + 17,655$	0.7346
5	Polynomial 3	$TSS = -6E+08*(Rrs\_645)^3 + 4E+06*(Rrs\_645)^2 + 6685,2*(Rrs\_645) + 29,723$	0.7452
6	Power	$TSS = 767,24*(Rrs\_645)^{0,4333}$	0.6339

The histogram of each wavelength shown in Fig 7, where in the images of the histogram can be seen the maximum frequency of reflectance for 412 nm, 531 nm, and 645 nm. The wavelength of 412 and the wavelength of 531 shows the reflectance value is more diffuse than the wavelength of 645, this shows that the wavelength of 645 has a detection scale that is sharper than other wavelengths, where the frequency of the reflectance value is more centralized.

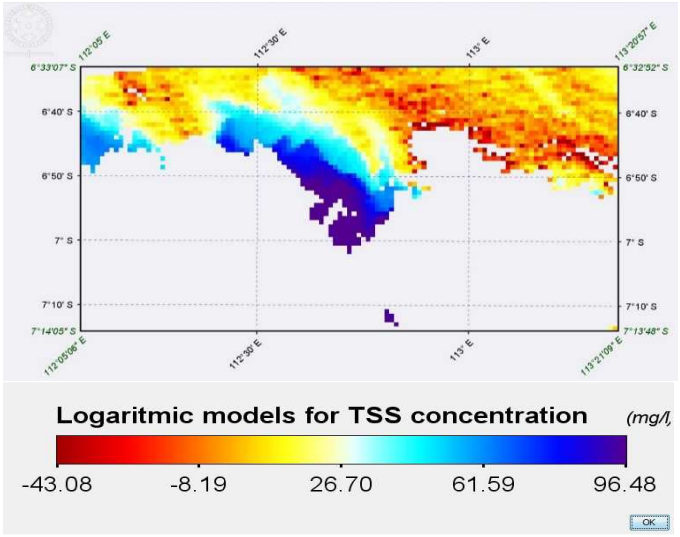

Fig 5. Thematic map of TSS concentration with logarithmic models

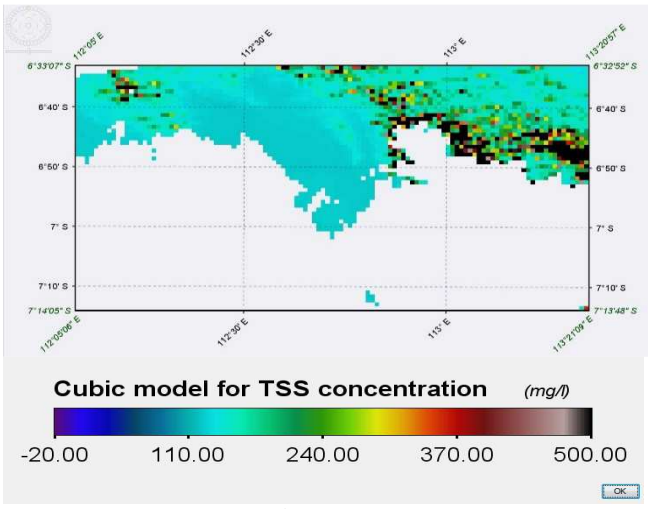

Fig 6. Thematic map of TSS concentration with cubic model

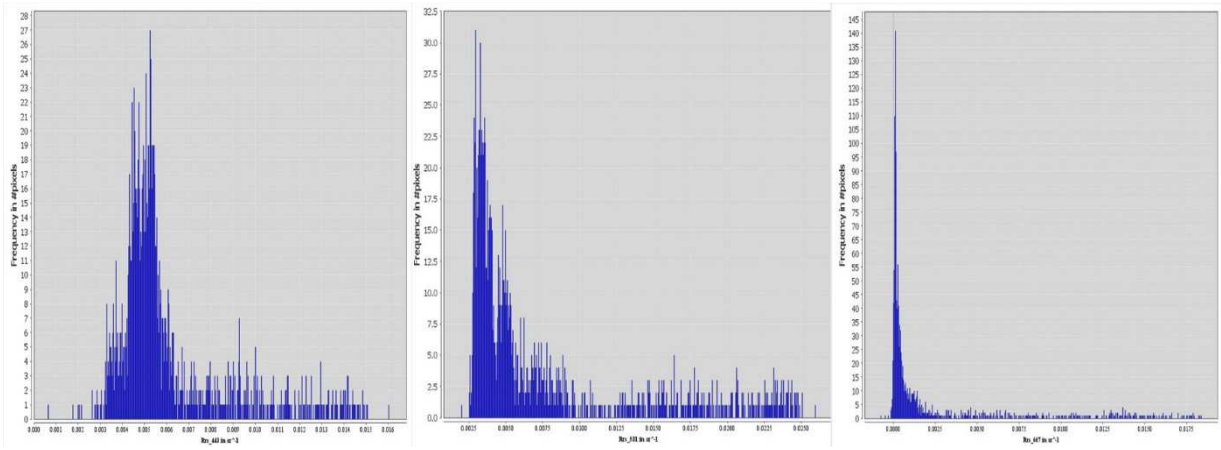

Fig 7. Histogram of the wavelength 412 nm, 531 nm and 645 nm at coast Ujung Pangkah Gresik

Subsequently, Table 4 is taken as a reference to a representative mathematical model for the calculation and mapping of TSS concentrations on the coast of Ujung Pangkah Gresik. The mathematical model used as an example here is a logarithmic model and a polynomial model degree 3 or cubic. The mapping results with SeaDASS for the logarithmic model are shown in Figure 5, while the cubic model is shown in Figure 6.

C. Validation of mathematical models

The validation of the models that have been selected that is a logarithmic model and cubic model, both of them then used as a model to calculate the remaining data of TSS data as a form of belief on the model already selected, while the available data can be seen in Table 5

TABLE V
TSS CONCENTRATION FOR VALIDATION PROCESS

Longitude	Latitude	TSS (mg/l)
112.80209^o	-6.83163^o	57.4
112.88413^o	-6.82683^o	52.8
112.95905^o	-6.81524^o	38.4
113.02217^o	-6.80547^o	23.9
113.14269^o	-6.78107^o	61.5

For the calculation of TSS values in logarithmic models and cubic models performed using reflectance values at 645 wavelengths which are extracted at the coordinates as shown in Table 5, and the results have presented in Table 6, which is the value of total suspended solids at 645 wavelengths for the cubic model and logarithmic.

TABLE VI
RESULT OF TSS CONCENTRATION AT CUBIC AND LOGARITHMIC

Cubic at 645 nm (mg/l)	Logarithmic at 645 nm (mg/l)	TSS (mg/l)
69.608	63.301	57.40
50.305	51.800	52.80
40.484	41.188	38.40
17.698	84.747	23.90
85.325	71.267	61.50

The results obtained for the TSS values in the cubic and logarithmic models are then analyzed for correlation of each other with the mathematical TSS value, and the results as shown in Table 7 can be seen that the correlation model can be taken is the correlation of cubic model with TSS insitu where the correlation value that obtained is 0.9568, this is mean that 95,68% of the data in TSS insitu can be explained with the calculated data of TSS from the cubic models.

TABLE VII
CORRELATION OF CUBIC AND LOGARITHMIC MODELS WITH TSS INSITU

	TSS from cubic models	TSS from logarithmic models	*TSS insitu (mg/l)*
TSS from cubic models	1		
TSS from logarithmic models	-0,1094	1	
TSS insitu (mg/l)	0,9568	-0,2459	1

Table 7 shows the correlation analysis of TSS concentrations obtained in the field with TSS obtained from the calculation of the polynomial algorithm degree 3 and the logarithmic algorithm. This is done to see which mathematical model algorithms are most relevant. Table 7 shows the cubic or polynomial model of degree 3 has conformity with the TSS in situ of 0.9568, while the logarithm shows -0.2459, so it can be said that the cubic algorithm 95.68% of the data obtained shows conformity with the field sample data

IV. CONCLUSIONS

The reflectance data from Aqua Modis satellite imagery is still relevant enough to be used as a variable in mapping the concentration of TSS value on the coast, where with this data combined with the TSS concentration value will be obtained mathematical model in some form which has coefficient of determination value with varying quantity. The variation formed by the R-value of the mathematical model will determine the suitability of the model against the mapping of TSS concentrations in the field. And from a series of proposed models it can be concluded that the cubic model has to be considerable significance if it compared with the other model shapes, whereas the corresponding

wavelength for this is 645 nm representing the red channel of the satellite image. The value result of the model if it compares with the TSS insitu on correlation analysis shows that the cubic model has the big proportion, so in the coastal area of Ujung Pangkah Gresik the changes of the suspended solid concentration have a probability cubic model that can be applied in the area for the need of forecasting

ACKNOWLEDGMENT

The authors are grateful to the Ministry of Technology and Higher Education who has provided scholarship funds through BPPDN so that the authors can complete this research well, also to fellow students of Civil Engineering UPN "Veteran" East Java which has a lot of help in the process of sampling data water in the field.

REFERENCES

[1] D. Wang *et al*., "Impact of sensor degradation on the MODIS NDVI time series," *Remote Sens. Environ.*, 2012.

[2] C. B. Schaaf *et al*., "First operational BRDF, albedo nadir reflectance products from MODIS," *Remote Sens. Environ.*, 2002.

[3] Y. Wang *et al*., "Assessment of biases in MODIS surface reflectance due to Lambertian approximation," *Remote Sens. Environ.*, 2010.

[4] J. Guang, Y. Xue, L. Yang, L. Mei, and X. He, "A method for retrieving land surface reflectance using MODIS data," *IEEE J. Sel. Top. Appl. Earth Obs. Remote Sens.*, 2013.

[5] X. Che, M. Feng, H. Jiang, J. Song, and B. Jia, "Downscaling MODIS surface reflectance to improve water body extraction," *Adv. Meteorol.*, 2015.

[6] V. Brando, A. Dekker, A. Marks, Y. Qin, and K. Oubelkheir, "Chlorophyll and suspended sediment assessment in a macrotidal tropical estuary adjacent to the Great Barrier Reef: Spatial and temporal assessment using remote sensing," *Coop. Res. Cent. Coast. Zo. Estuary Waterw. Manag. - Tech. Rep. 74*, pp. 1–128, 2006.

[7] K. Nieto and F. Mélin, "Variability of chlorophyll-a concentration in the Gulf of Guinea and its relation to physical oceanographic variables," *Prog. Oceanogr.*, vol. 151, pp. 97–115, 2017.

[8] T. Lacava *et al.*, "Evaluation of MODIS—Aqua Chlorophyll-a Algorithms in the Basilicata Ionian Coastal Waters," *Remote Sens.*, vol. 10, no. 7, p. 987, Jun. 2018.

[9] M. A. Cane *et al*., "Twentieth-century sea surface temperature trends," *Science (80-.).*, 1997.

[10] C. Jian, Y. O. U. Xiaobao, X. Yiguo, Z. Ren, W. Gongjie, and B. A. O. Senliang, "A performance evaluation of remotely sensed sea surface salinity products in combination with other surface measurements in reconstructing three-dimensional salinity fields," vol. 36, no. 7, pp. 15–31, 2017.

[11] H. Loisel *et al.*, "Variability of suspended particulate matter concentration in coastal waters under the Mekong's influence from ocean color (MERIS) remote sensing over the last decade," *Remote Sens. Environ.*, vol. 150, pp. 218–230, Jul. 2014.

[12] H. Xi, Y. Zhang, H. Xi, and Y. Zhang, "Total suspended matter observation in the Pearl River estuary from in situ and MERIS data," *Env. Monit Assess*, vol. 177, pp. 563–574, 2011.

[13] D. Kyryliuk and S. Kratzer, "Total suspended matter derived from MERIS data as indicator for coastal processes in the Baltic Sea."

[14] E. Kari, S. Kratzer, J. M. Beltrán-Abaunza, E. T. Harvey, and D. Vaičiūtė, "Retrieval of suspended particulate matter from turbidity – model development, validation, and application to MERIS data over the Baltic Sea," *Int. J. Remote Sens.*, vol. 38, no. 7, pp. 1983–2003, Apr. 2017.

[15] T. Hariyanto, T. C. Krisna, C. B. Pribadi, A. Kurniawan, B. M. Sukojo, and M. Taufik, "Evaluation of Total Suspended Sediment (TSS) Distribution Using ASTER, ALOS, SPOT-4 Satellite Imagery in 2005-2012," *IOP Conf. Ser. Earth Environ. Sci.*, vol. 98, no. 1, p. 012026, Dec. 2017.

[16] S. Lehner, I. Anders, and G. Gayer, "High Resolution Maps Of Suspended Particulate Matter Concentration In The German Bight," *EARSeL eProceedings 3*, vol. 1, 2004.

[17] J. J. Walker, K. M. De Beurs, R. H. Wynne, and F. Gao, "Evaluation of Landsat and MODIS data fusion products for analysis of dryland forest phenology," *Remote Sens. Environ.*, 2012.

[18] M. Feng, C. Huang, S. Channan, E. F. Vermote, J. G. Masek, and J. R. Townshend, "Quality assessment of Landsat surface reflectance products using MODIS data," *Comput. Geosci.*, 2012.

[19] Emiyati, A. K. S. Manoppo, and S. Budhiman, "Estimation on the concentration of total suspended matter in Lombok Coastal using Landsat 8 OLI, Indonesia," *IOP Conf. Ser. Earth Environ. Sci.*, vol. 54, no. 1, p. 012073, Jan. 2017.

[20] C. Petus, G. Chust, F. Gohin, D. Doxaran, J. M. Froidefond, and Y. Sagarminaga, "Estimating turbidity and total suspended matter in the Adour River plume (South Bay of Biscay) using MODIS 250-m imagery," *Cont. Shelf Res.*, vol. 30, no. 5, pp. 379–392, 2010.

[21] E. Robert *et al.*, "Monitoring water turbidity and surface suspended sediment concentration of the Bagre Reservoir (Burkina Faso) using MODIS and field reflectance data," *Int. J. Appl. Earth Obs. Geoinf.*, 2016.

[22] L. A. Karondia and L. M. Jaelani, "Validasi Algoritma Estimasi Total Suspended Solid dan Chl-A Pada Citra Satelit Aqua Modis dan Terra Modis dengan Data In Situ (Studi Kasus : Laut Utara Pulau Jawa)," *Geoid*, vol. 11, no. 1, pp. 46–51, 2015.

[23] R. Asadpour, L. H. San, M. M. Alashloo, and S. Y. Moussavi, "A Statistical Model for Mapping Spatial Distribution of Total Suspended Solid from THEOS Satellite Imagery Over Penang Island, Malaysia," vol. 8, no. 1, pp. 271–276, 2012.

[24] T. E. Baxter, "Standard Operating Procedure Total Dissolved Solids by Gravimetric Determination," 2017.